Regular Article

blood

THROMBOSIS AND HEMOSTASIS

Hyperfibrinolysis increases blood–brain barrier permeability by a plasmin- and bradykinin-dependent mechanism

Oscar A. Marcos-Contreras,[1,*] Sara Martinez de Lizarrondo,[1,*] Isabelle Bardou,[1] Cyrille Orset,[1] Mathilde Pruvost,[1] Antoine Anfray,[1] Yvann Frigout,[1] Yannick Hommet,[1] Laurent Lebouvier,[1] Joan Montaner,[2] Denis Vivien,[1,3,*] and Maxime Gauberti[1,4,*]

[1]INSERM Unité 919, Serine Proteases and Pathophysiology of the Neurovascular Unit, Cyceron, Université de Caen Normandy (UNICAEN) Caen, France; [2]Neurovascular Research Laboratory, Vall d'Hebron Research Institute, Barcelona, Spain; [3]Department of Cell Biology, and [4]Department of Diagnostic Imaging and Interventional Radiology, Medical Center, Caen University Hospital, Caen, France

Key Points

- Hydrodynamic transfection of plasmids encoding for plasminogen activators leads to a hyperfibrinolytic state in mice.
- Hyperfibrinolysis increases BBB permeability via a plasmin- and bradykinin-dependent mechanism.

Hyperfibrinolysis is a systemic condition occurring in various clinical disorders such as trauma, liver cirrhosis, and leukemia. Apart from increased bleeding tendency, the pathophysiological consequences of hyperfibrinolysis remain largely unknown. Our aim was to develop an experimental model of hyperfibrinolysis and to study its effects on the homeostasis of the blood–brain barrier (BBB). We induced a sustained hyperfibrinolytic state in mice by hydrodynamic transfection of a plasmid encoding for tissue-type plasminogen activator (tPA). As revealed by near-infrared fluorescence imaging, hyperfibrinolytic mice presented a significant increase in BBB permeability. Using a set of deletion variants of tPA and pharmacological approaches, we demonstrated that this effect was independent of *N*-methyl-D-aspartate receptor, low-density lipoprotein–related protein, protease-activated receptor-1, or matrix metalloproteinases. In contrast, we provide evidence that hyperfibrinolysis-induced BBB leakage is dependent on plasmin-mediated generation of bradykinin and subsequent activation of bradykinin B2 receptors. Accordingly, this effect was prevented by icatibant, a clinically available B2 receptor antagonist. In agreement with these preclinical data, bradykinin generation was also observed in humans in a context of acute pharmacological hyperfibrinolysis. Altogether, these results suggest that B2 receptor blockade may be a promising strategy to prevent the deleterious effects of hyperfibrinolysis on the homeostasis of the BBB. (*Blood*. 2016;128(20):2423-2434)

Introduction

In a large number of clinical situations, the endogenous fibrinolytic system may become chronically activated and lead to a hyperfibrinolytic state. For example, recent studies demonstrated that 57% of trauma patients[1] and 60% of patients with cirrhosis[2] present with hyperfibrinolysis, which is associated with poor outcomes. Studies in patients presenting with out-of-hospital cardiac arrest[3] and acute promyelocytic leukemia[4] reported similar results. Iatrogenic hyperfibrinolysis can also be induced in the treatment of acute ischemic stroke, myocardial infarction, pulmonary embolism, or limb ischemia by systemic administration of plasminogen activators (such as tissue-type plasminogen activator [tPA]). In all these situations, hyperfibrinolysis is the consequence of an imbalance between profibrinolytic (tPA and urokinase) and antifibrinolytic (such as plasminogen activator inhibitors, α2-antiplasmin, or thrombin-activatable fibrinolysis inhibitor) factors.[5] The most evident pathological effect of hyperfibrinolysis is an increased bleeding tendency.[6] Nevertheless, the lack of relevant experimental models limits our understanding of this complex pathological situation. Because recent studies demonstrated that hyperfibrinolysis is involved in numerous diseases, a deeper understanding of its pathophysiological roles would be of potential clinical interest.

In the present study, we developed an experimental model of hyperfibrinolysis, using a chronic overexpression of a plasminogen activator (tPA) in the liver and subsequent release in the circulation. This was achieved using hydrodynamic transfections of plasminogen activators containing plasmids in mice. After characterization of this model, we focused our study on the effects of hyperfibrinolysis on the integrity of the blood–brain barrier (BBB). We found that hyperfibrinolytic mice presented an increased permeability of the BBB. Pharmacological and molecular investigations allowed us to demonstrate that this mechanism was dependent on plasmin, bradykinin generation, and bradykinin B2 receptor activation. Then,

Submitted 15 March 2016; accepted 6 August 2016. Prepublished online as *Blood* First Edition paper, 16 August 2016; DOI 10.1182/blood-2016-03-705384.

*O.A.M.-C., S.M.d.L., D.V., and M.G. contributed equally to this study.

The online version of this article contains a data supplement.

There is an Inside *Blood* Commentary on this article in this issue.

The publication costs of this article were defrayed in part by page charge payment. Therefore, and solely to indicate this fact, this article is hereby marked "advertisement" in accordance with 18 USC section 1734.

we validated our preclinical data in the clinical setting by showing that hyperfibrinolysis induced by tPA infusion in patients with stroke also led to a significant bradykinin generation.

Methods

An extended material and methods section is available as an online supplement on the *Blood* Web site.

Hydrodynamic transfection

Hydrodynamic transfections were performed as previously described[7]: mice were injected with 100 μg engineered pLIVE encoding wild-type rat tPA (pLIVE-tPA), tPA mutants (tPA-K2* and Δ-Finger), tPA–green fluorescent protein (tPA-GFP) fusion protein, tPA–luciferase fusion protein (tPA-Luc), or pLIVE plasmid alone (pLIVE-0) as a control (supplemental Figure 1). Briefly, a large volume (10% of body weight) of plasmid-containing saline buffer (0.9% NaCl) was injected in the tail vein in less than 5 seconds. A negligible mortality was observed during this procedure (<3%). To measure BBB permeability, 200 μL Evans blue (EB) at 0.8% in phosphate-buffered saline was injected intravenously 2 hours before euthanasia and 48 hours after hepatic transfection, and the organs were imaged with near-infrared fluorescence (NIRF), as described in "Ex vivo NIRF." Different treatments were injected as follows, after hydrodynamic transfection: ε-aminocaproic acid (EACA) and tranexamic acid (600 mg/kg, subcutaneously [s.c.] every 12 hours) and aprotinin (0.5 mg/kg intraperitoneally every 12 hours), SCH-79797 (1 mg/kg s.c. every 12 hours), MK801 (2 mg/kg s.c., every 12 hours), CP-471474 (1 mg/kg s.c. every 12 hours), and icatibant (0.5 mg/kg s.c., every 12 hours). Blood sampling was performed by retro-orbital or intracardial puncture in anesthetized mice at different points. Blood was anticoagulated using citrate.

Ex vivo NIRF

NIRF imaging experiments were performed using a PhotonIMAGER (Biospace, Paris, France), as previously described,[8,9] with several modifications. To allow the detection of EB at 650 nm, 5 mice per group were injected with EB 48 hours after pLIVE injection. EB was allowed to circulate for 120 minutes, and then deeply anesthetized mice were transcardially perfused with cold heparinized saline (15 mL/min; 75 mL) before organ removal. Excitation time was set at 10 seconds. The photon count of the whole brain, heart, liver, left kidney, or left hind limb was measured ex vivo and normalized at 100% for pLIVE control animals.

Results

Hydrodynamic transfection of pLIVE-tPA induces sustained secretion of active tPA in the circulation

We hypothesized that an artificial chronic overexpression of tPA by liver cells and its subsequent release in the circulation may mimic hyperfibrinolytic state. Thus, we first generated a set of expression vectors (pLIVE) encoding for rat tPA driven by a liver-specific promoter (pLIVE-tPA, pLIVE-tPA-GFP, and pLIVE-tPA-Luc) (Figure 1A). The liver was transfected in vivo by a hydrodynamic injection of 100 μg pLIVE-tPA constructs or pLIVE empty vector as control (pLIVE-0). Then, we performed zymography assays, immunohistological analyses, and bioluminescence imaging of the major organs 48 hours after hydrodynamic transfection to measure tPA expression and activity (Figure 1B). Importantly, rat tPA interacts with the mouse fibrinolytic system, including mouse PAI-1, and presents an increased activity in mouse plasma compared with human tPA (supplemental Figures 2–5).

Immunofluorescence analyses in tPA-GFP-transfected mice revealed a tissue-specific expression of tPA in the liver (Figure 1C; supplemental Figure 6) without significant expression in other cells or organs, including the brain. This was confirmed by zymography assays performed using liver tissue homogenates (Figure 1D), also addressing the fact that the tPA produced by the liver was proteolytically active. Using hydrodynamic transfection of a tPA–luciferase construct, we were able to visualize tPA overexpression in a noninvasive manner (Figure 1E). After injection of coelenterazine (a bioluminescent luciferase substrate), we detected luciferase activity specifically in the liver, further confirming the specificity of the expression of the pLIVE-tPA-Luc construct (Figure 1E). Importantly, mice transfected with the control pLIVE-0 plasmid did not show a bioluminescence signal. This was also confirmed ex vivo in exsanguinated organs (brain, kidney, heart, and liver), showing that tPA was only overexpressed in the liver (Figure 1F; supplemental Figure 7). Moreover, a longitudinal study of tPA expression levels was performed in pLIVE-tPA-Luc-transfected mice (from 1 to 69 days), showing that tPA overexpression lasts for more than 7 days (supplemental Figure 8). Altogether, these results demonstrated that hydrodynamic transfection was effective in inducing sustained expression of active tPA by the liver.

Then, we investigated whether this liver overexpression leads to higher tPA plasmatic levels. To this aim, we performed fibrin-agar zymography of plasma from pLIVE-0- and pLIVE-tPA-transfected mice before and after hepatic transfection. We observed a plasmatic overexpression of tPA as soon as 24 hours after hepatic transfection in the pLIVE-tPA mice, which was not present in the same animals before transfection, and in pLIVE-0-transfected mice (Figure 1G). This overexpression was especially significant during the first week, revealing free and active tPA in the circulation of transfected animals (Figure 1H). The highest plasmatic level of free active tPA was reached around 48 hours after transfection (Figure 1H). Plasmatic concentrations of active tPA in all successfully injected mice were measured between 1.5 and 4.5 nM at 48 hours after transfection by solid-phase fibrinolytic assay (data not shown).

Altogether, these results demonstrated that hydrodynamic transfection of pLIVE-tPA leads to a chronic plasmatic secretion of tPA.

Hyperfibrinolysis induces BBB permeabilization

To investigate whether this increased plasmatic concentration of tPA leads to a hyperfibrinolytic state, we took blood samples from pLIVE-0- and pLIVE-tPA-transfected mice 48 hours after hydrodynamic transfection and performed euglobulin lysis time assays. As illustrated in Figure 2A-B, pLIVE-tPA-transfected mice presented a 36% shorter euglobulin lysis time than pLIVE-0-transfected mice. These results demonstrated that the chronic plasmatic secretion of tPA triggered by hydrodynamic transfection of pLIVE-tPA leads to a hyperfibrinolytic state.

We thus investigated whether hyperfibrinolysis could affect BBB homeostasis. For that purpose, we injected EB, a fluorescent dye that binds to albumin and cannot cross the intact BBB. At the time of maximal plasmatic tPA levels (48 hours after hydrodynamic transfection), mice were exsanguinated 2 hours after EB injection, using an intracardial perfusion of cold heparinized saline, and the brains and spinal cords were collected. We measured fluorescence of the brains and spinal cord to detect BBB leakage (Figure 2C). Visualization of EB extravasation revealed significant BBB leakage in hyperfibrinolytic mice (pLIVE-tPA), whereas the BBB remained impermeable to EB in control (pLIVE-0) animals (Figure 2D, right and left, respectively). Therefore, these results demonstrated that hyperfibrinolysis induces BBB permeabilization to large molecules (molecular weight of EB

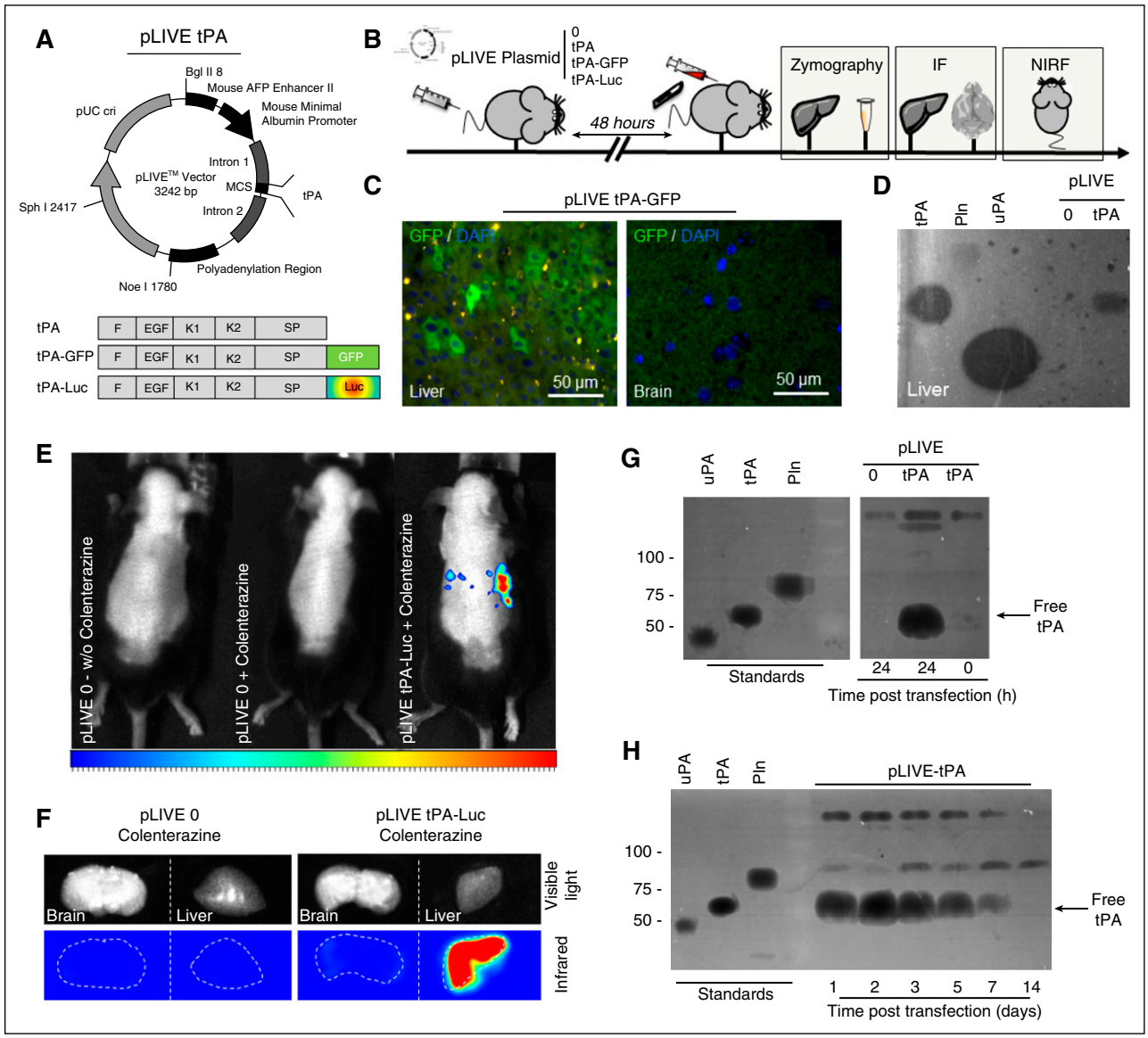

Figure 1. Development and characterization of a tPA-hepatic transfection model that promotes chronic hyperfibrinolytic state in mice. (A) Schematic representations of the generated pLIVE-tPA constructs, including the complete tPA sequence (5 domains: Finger [F], epithelial growth factor [EGF], kringle 1 and 2 [K1, K2], and serine protease [SP]). tPA-GFP and tPA-Luc plasmids contain the whole tPA sequence with the fusion proteins green fluorescent protein (GFP) and luciferase (Luc), respectively. (B) Schematic representation of the experimental timeline including in vitro (zymography), in vivo (bioluminescence), and ex vivo (immunofluorescence [IF] and NIRF) experiments. (C) Fluorescence images of pLIVE-tPA-GFP-transfected animals showing tPA overexpression (GFP labeling) in the liver, and not the brain, at 48 hours after transfection. (D) Fibrin-agar zymography of liver homogenates of pLIVE-0- and pLIVE-tPA-transfected animals. (E) In vivo luminescence in pLIVE-tPA-Luc-transfected mice after intraperitoneal coelenterazine (luciferase substrate) injection (48 hours after transfection). (F) Representative ex vivo images of the liver and brain from pLIVE-0- and pLIVE-tPA-Luc-transfected mice, revealing significant luminescence only in the liver of pLIVE-tPA-Luc-transfected mice. (G) Fibrin-agar zymography from plasma samples of pLIVE-0- and pLIVE-tPA-transfected mice before and 24 hours after hepatic transfection. Only pLIVE-tPA mice presented significant levels of free circulating tPA. (H) Representative fibrin-agar zymography of a pLIVE-tPA-transfected mice plasma, which demonstrates the presence of free plasmatic tPA several days after the transfection. 4′,6-diamidino-2-phenylindole (DAPI, blue) was used as a nuclear marker; tPA, urokinase plasminogen activator (uPA), and Pln (plasmin) were used as standards in the zymographies. All the images presented are representative of at least 5 biological replicates of the experiment.

bound to mouse serum albumin is ~67 kDa). This effect is not mediated by the hydrodynamic injection protocol itself, as mice transfected with an empty pLIVE-0 vector did not show EB extravasation (Figure 2D). Quantification of EB fluorescence using NIRF, as recently described,[8,9] confirmed significantly higher EB concentrations in the brains of hyperfibrinolytic animals compared with controls (Figure 2E-F). Interestingly, we observed that EB extravasation was restricted to the encephalon, sparing the spinal cord (Figure 2G-H). Epifluorescence microscopy confirmed EB extravasation in hyperfibrinolytic animals as a red diffused staining near the vessels in the cortex and cerebellum (Figure 2I). Consistent with the results on Figure 2G-H, no EB was detected in the spinal cord of hyperfibrinolytic animals (Figure 2I).

BBB leakage is mediated by plasmin generation

Thereafter, we investigated the molecular pathways responsible for BBB leakage in hyperfibrinolytic mice. To study the possibility that tPA induces BBB leakage by its interactions with *N*-methyl-D-aspartate (NMDA) or low-density lipoprotein related (LRP) receptors,[10,11] we used recently generated tPA mutants[12] that we included into pLIVE vectors: the K2*-tPA, consisting in a single-point mutation in the

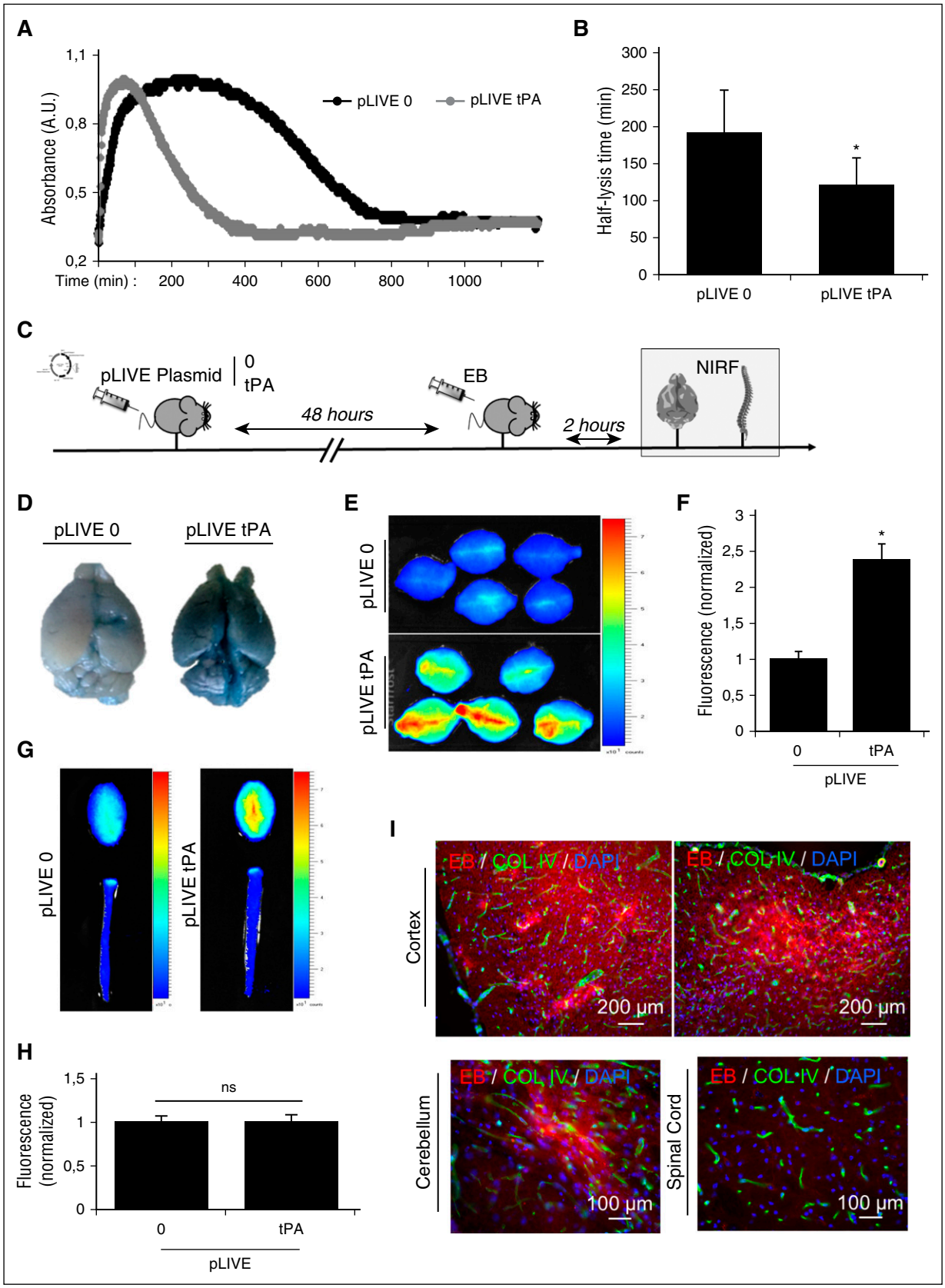

Figure 2. Hyperfibrinolytic state induces BBB leakage of EB. (A) Representative euglobulin lysis time assay from plasma samples of pLIVE-0- and pLIVE-tPA-transfected mice (harvested 48 hours after hydrodynamic transfection). (B) Corresponding quantification of the half-lysis time (n = 5 per group). (C) Experimental design performed to study BBB permeability using NIRF techniques. EB extravasation was measured ex vivo 48 hours after pLIVE (0 or tPA) transfection in the brain and the spinal cord. (D) Representative pictures of ex vivo brains after pLIVE (0 or tPA) transfection. (E) Brain EB permeability was quantified by NIRF. (F) Normalized mean fluorescence quantification of D (n = 5 per group). (G) Ex vivo representative images of the brain and spinal cords after pLIVE transfection. (H) Normalized mean fluorescence quantification of spinal cord EB extravasation (n = 5 per group). (I) Representative epifluorescence images of pLIVE-tPA-transfected animals, showing EB extravasation (red) in the cortex and the cerebellum, but not in the spinal cord. *$P < .05$ vs control; ns = nonsignificant differences.

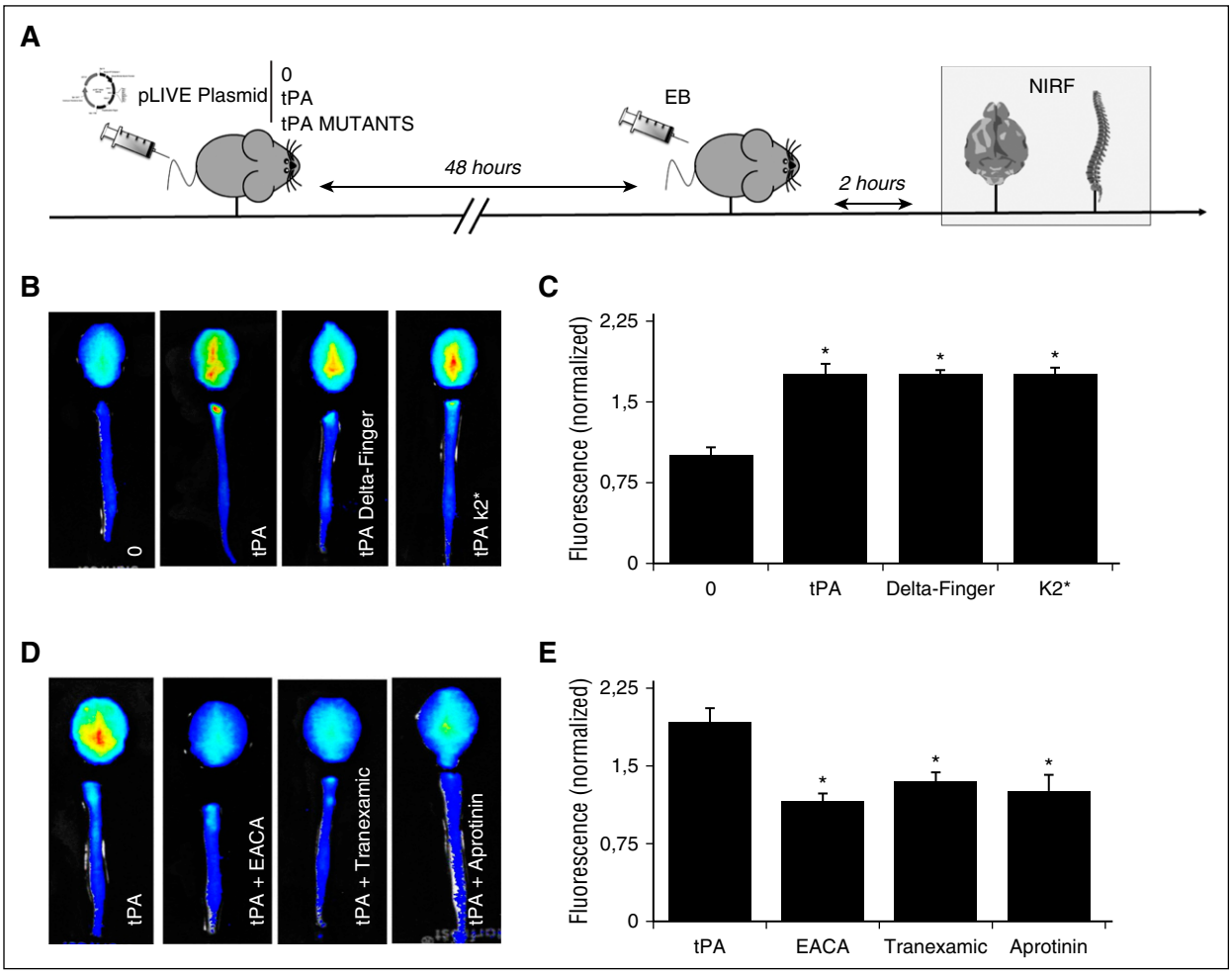

Figure 3. Hyperfibrinolysis induces BBB leakage in a plasmin-dependent manner. (A) Design of the experiments performed to study BBB permeability, using NIRF techniques. EB extravasation was measured 48 hours after pLIVE (0, wild-type or mutated tPA plasmids) hydrodynamic transfection in the brain and the spinal cord. (B) All pLIVE-tPA constructions (wild-type and tPA mutations in Finger [Δ-Finger] and Kringle-2 [K2*] domains) promoted EB extravasation in the brain compared with pLIVE-0 (control). (C) Normalized mean fluorescence quantification of B (n = 5 per group). (D) BBB leakage is dependent on plasmin generation, as inhibition of the activation of plasminogen into plasmin (by EACA and tranexamic) or inhibition of plasmin activity (by aprotinin) prevented EB extravasation in mice with hyperfibrinolysis. *$P < .05$ vs control.

kringle 2 domain of tPA, preventing its interaction with NMDA-receptor (R)[12] and the Δ-Finger-tPA, consisting of a tPA deleted of its finger domain that cannot interact with the LRP receptor, as well as the control (pLIVE-0) and the native pLIVE-tPA plasmid. We injected EB intravenously (200 μL at 0.8%) 48 hours after transfection of the different tPA mutants and measured its extravasation by NIRF (Figure 3A). All tPA- and tPA mutant–transfected mice presented equal extravasation of EB compared with the control group (pLIVE-0), arguing against a LRP or NMDA-R-mediated mechanism (Figure 3B-C). We subsequently hypothesized that the mechanism by which hyperfibrinolysis induces BBB disruption could be mediated by plasmin, in line with previous studies that have shown the implication of plasmin in BBB impairment.[13] To test this hypothesis, we treated pLIVE-tPA-transfected animals with antifibrinolytic compounds that block plasmin generation and/or activity. We used EACA, tranexamic acid (both lysine analogs that block the conversion of plasminogen into plasmin by tPA), or aprotinin (a plasmin inhibitor). Interestingly, in all pLIVE-tPA-transfected animals that received antifibrinolytic treatments, EB extravasation was reduced to levels comparable with pLIVE-0-transfected mice (Figure 3D-E). Altogether, these results demonstrated that hyperfibrinolysis induces BBB leakage by a plasmin-dependent mechanism.

Hyperfibrinolysis-induced BBB leakage is independent of inflammatory processes or neuronal death

Thereafter, we made the hypothesis that the BBB leakage could be linked to either pro-inflammatory or/and proneurotoxic effects of the tPA–plasminogen axis.[14] To test this hypothesis, we first analyzed the morphology and number of microglial cells in the brain parenchyma of control and pLIVE-tPA-transfected mice by immunohistochemistry. We observed no significant differences between pLIVE-tPA and control (pLIVE-0) groups in terms of morphology (Figure 4A) or number of microglial cells (Iba-1–positive) (Figure 4B). Then, we measured the brain expression (quantitative polymerase chain reaction) of 2 cytokines (interleukin 1-β and tumor necrosis factor), known to be upregulated in neuroinflammatory situations. We did not find differences in the expression levels between pLIVE-0- and pLIVE-tPA-transfected mice, respectively (Figure 4C-D). Third, we analyzed the expression/regulation of VCAM-1 and ICAM-1, 2 key adhesion molecules during neuroinflammatory processes,[15] by immunohistochemistry (Figure 4E-F), quantitative polymerase chain reaction (Figure 3G-H), and molecular magnetic resonance imaging, a recently developed method that uses iron oxide microparticles targeted against VCAM-1 to reveal activated endothelial cells in the brain in an

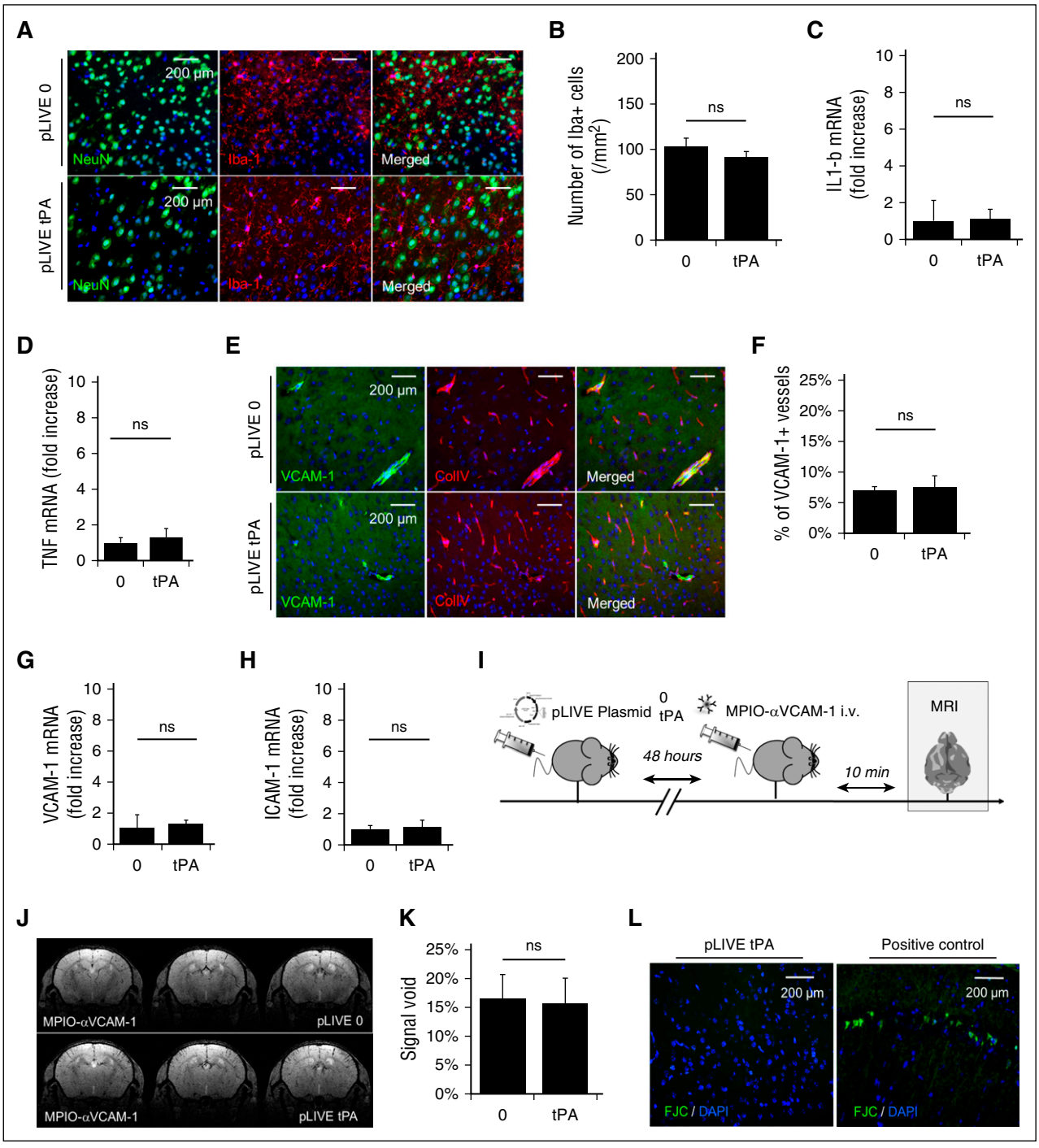

Figure 4. Inflammation does not play a role in BBB leakage after tPA overexpression. All experiments were performed 48 hours after hydrodynamic transfection of pLIVE-tPA or pLIVE-0 plasmids. (A) Immunofluorescence images of pLIVE-0- and pLIVE-tPA-transfected animals, showing that microglial cells (expressing ionized calcium binding adaptor molecule 1 [Iba-1], red) remain ramified (ie, not activated) in mice presenting a hyperfibrinolytic state. (B) Quantification of Iba-1–positive cells (n = 5 per group). (C) Interleukin 1-β expression levels (mRNA) in brain lysates in pLIVE-0- and tPA-transfected mice (n = 5 per group). (D) Tumor necrosis factor expression levels in brain lysates in pLIVE-0- and tPA-transfected mice (n = 5 per group). (E) Fluorescence images of pLIVE 0- and tPA-transfected animals showing that brain VCAM-1 expression (green) levels are not modified after plasmatic tPA overexpression. (F) Quantification of VCAM-1–positive endothelial cells in E (n = 5 per group). (G) VCAM-1 mRNA expression levels in brain lysates in pLIVE-0- and pLIVE-tPA-transfected mice (n = 5 per group). (H) ICAM-1 mRNA expression levels in brain lysates in pLIVE-0- and tPA-transfected mice (n = 5 per group). (I) Experimental design performed to study VCAM-1 expression using ultrasensitive molecular magnetic resonance imaging technique. Imaging was performed 20 minutes after iron oxide microparticles-α–VCAM-1 injection. (J) Representative magnetic resonance image after iron oxide microparticles–VCAM-1 administration in control and tPA-transfected mice. (K) Mean signal void iron oxide microparticles–VCAM-1 levels of J (n = 5 per group). (L) Using Fluoro-Jade C staining (green), no neuronal cell-death was detected 48 hours after pLIVE-tPA injection (left) compared with a positive control (transient bilateral occlusion of the common carotid arteries model; right), arguing against the implication of neuronal damage in tPA-induced BBB leakage. 4′,6-diamidino-2-phenylindole (DAPI; blue) was used as a nuclear marker, collagen IV (Coll IV; red) as an endothelial marker, and NeuN (green) as a neuronal marker. FJC, fluoro-jade C; Iba+, ; IL, interleukin; MPIO, iron oxide microparticles; MRI, magnetic resonance imaging; ns, nonsignificant differences.

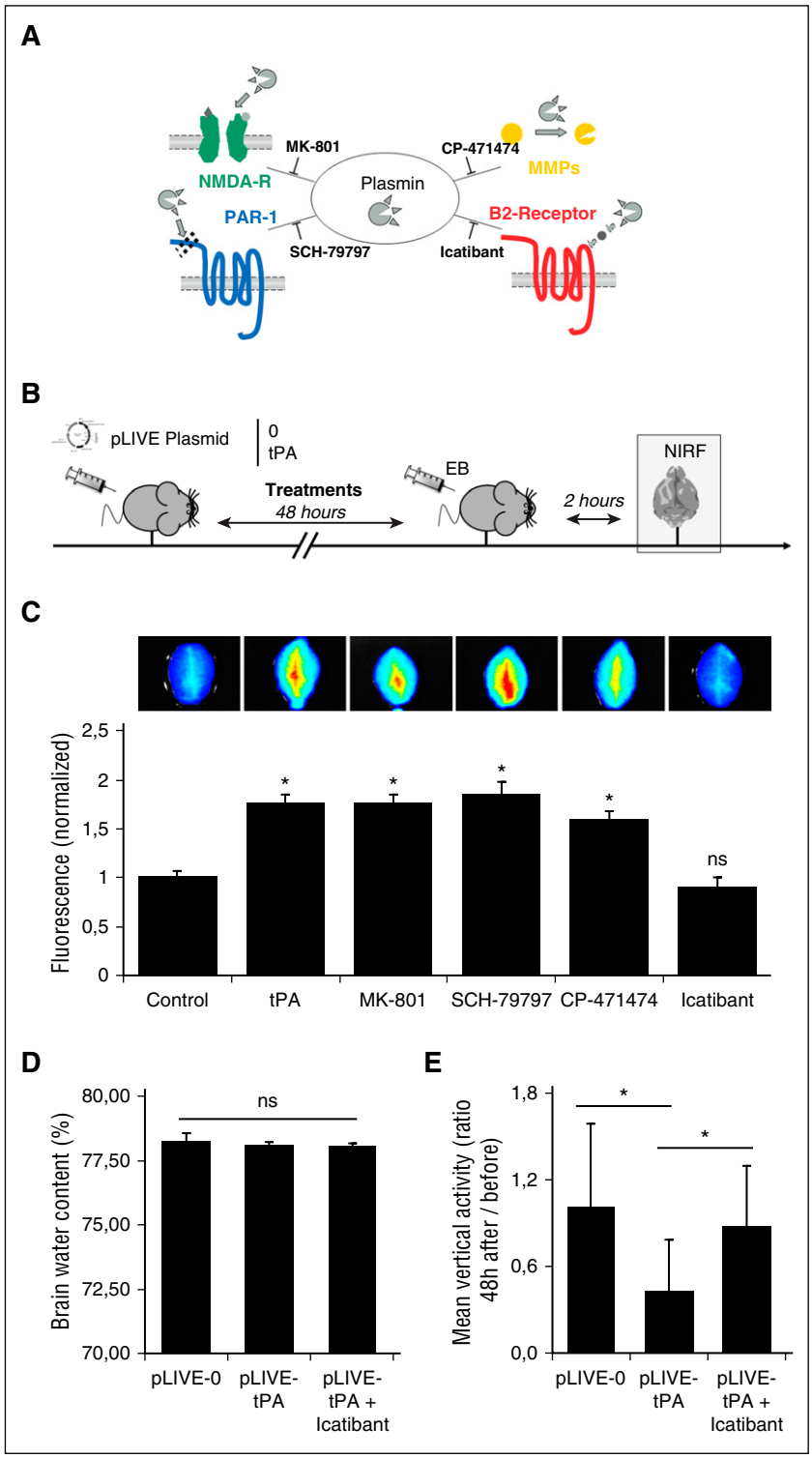

Figure 5. Plasmin induces BBB leakage in a bradykinin B2 receptor–dependent manner. (A) Schematic representation of the known effects of plasmin and corresponding inhibitors. (B) Experimental design performed to study BBB permeability, using NIRF techniques. EB extravasation was measured ex vivo 48 hours after pLIVE (0 or tPA) transfection in the brain. (C) Fluorescence images of pLIVE-tPA-transfected animals, showing that neither the blockade of NMDA-R (MK-801) or PAR-1 (SCH-79797) nor matrix metalloproteinases (CP-471474) prevented BBB leakage (n = 5 per group). Only icatibant (bradykinin B2 receptor inhibitor) prevented plasmin-dependent BBB leakage in hyperfibrinolytic mice. (D) Mean brain water contents (%) at +48 hours of pLIVE-0- and pLIVE-tPA-transfected mice treated or not with icatibant (0.5 mg every 12 hours; n = 10 per group). (E) Mean spontaneous locomotor activities (vertical moves), expressed as ratios between +48 hours and immediately before hydrodynamic transfections of pLIVE-0- and pLIVE-tPA-transfected mice treated or not with icatibant (0.5 mg every 12 hours; n = 10 per group). *$P < .05$ vs control; ns, nonsignificant differences.

ultrasensitive manner (Figure 3I-K).[16-18] Immunohistochemistry, quantitative polymerase chain reaction, and magnetic resonance imaging for VCAM-1 showed no difference between the 2 groups (Figure 4E-K). Finally, we also excluded the possibility that the plasmin-induced BBB leakage was mediated by neuronal cell death, as Fluoro-Jade C staining, known to label degenerating neurons, was negative in hyperfibrinolytic animals (Figure 4L). Altogether, these results demonstrated that hyperfibrinolysis-induced BBB leakage occurs independent of neuroinflammation or neuronal cell death.

Plasmin induces BBB disruption in a bradykinin B2 receptor–dependent manner

Plasmin is known to have pleiotropic actions in the neurovascular unit: it can act directly on NMDA-R[19] and activate matrix

metalloproteinases[20-22] or protease-activated receptor-1[19,23] (Figure 5A). To further elucidate the mechanism by which plasmin induces the observed BBB leakage, we administered direct inhibitors of the different plasmin substrates to pLIVE-tPA-transfected mice (Figure 5B). Interestingly, we found that MK-801 (an inhibitor of NMDA-R), SCH-79797 (an inhibitor of protease activated receptor-1), and CP-474471 (a large spectrum matrix metalloproteinase inhibitor) failed to prevent BBB leakage (Figure 5C). Because the plasmin-dependent increase in BBB permeability observed in hyperfibrinolytic mice appeared independent of established plasmin substrates, we looked for other candidates. Notably, there are only a few agents affecting BBB permeability described in the literature. Among them, bradykinin and its related peptides are the most characterized and are able to permeabilize the BBB through B2-receptor activation on endothelial cells.[24] Therefore, to investigate whether plasmin acts by generating bradykinin, we injected icatibant (a clinically available, specific inhibitor of bradykinin B2 receptor) in hyperfibrinolytic mice. As shown in Figure 5C, icatibant completely prevented EB extravasation, reducing the levels of brain fluorescence back to the level of controls. These results proved that blocking bradykinin B2 receptor activation prevents BBB leakage in hyperfibrinolytic mice.

Then, we investigated whether the hyperfibrinolytic state influences vascular permeability in other vascular beds (supplemental Figure 9). Our data revealed that hyperfibrinolysis increases vascular permeability in the hind limb, suggesting increasing permeability of skin capillaries. In contrast, no difference was observed in the kidney and in the heart. Consistent with a bradykinin B2 receptor–dependent mechanism, vascular permeability in the hind limbs was restored to a control value in icatibant-treated mice.

We also wanted to investigate whether hyperfibrinolysis influences brain edema and neurological function through bradykinin B2 receptor activation. To this aim, we first measured the brain water content 24 and 48 hours after hydrodynamic transfection of pLIVE-0 or pLIVE-tPA in mice treated with either saline or icatibant. No difference was observed between pLIVE-0- and pLIVE-tPA-transfected mice treated or not with icatibant, suggesting hyperfibrinolysis alone does not induce significant brain edema (Figure 5D; supplemental Figure 10). Next, we measured the spontaneous locomotor activity (vertical activity) of pLIVE-0- and pLIVE-tPA-transfected mice, using an automated system. Interestingly, pLIVE-tPA-transfected mice showed a reduced vertical activity compared with pLIVE-0-transfected mice (Figure 5E). Moreover, treatment with a B2 receptor antagonist (icatibant) of pLIVE-tPA-transfected mice restored vertical activity, impaired by the hyperfibrinolytic status, to the same level as pLIVE-0-transfected mice (Figure 5E). Importantly, other physiological variables such as temperature, blood pressure, heart rate, hematocrit, and weight were not significantly different between the experimental groups (supplemental Figure 11; supplemental Table 1). Altogether, these results showed that hyperfibrinolysis impairs spontaneous locomotor activity in mice by a bradykinin B2 receptor–dependent mechanism. It should, however, be acknowledged that we were not able to demonstrate elevated bradykinin plasma levels in hyperfibrinolytic mice by enzyme-linked immunosorbent assay (data not shown), probably because of the very short half-life of bradykinin in mice.

tPA-driven plasminogen activation induces bradykinin generation

Altogether, the results mentioned here suggested that increased chronic levels of plasmatic tPA lead to bradykinin generation by a plasmin-dependent mechanism, ultimately leading to B2 receptor activation and increased BBB permeability. To corroborate this molecular cascade, we first incubated recombinant high–molecular weight kininogen (HMWK, the circulating precursor of bradykinin), tPA, plasminogen, tPA+plasminogen, or tPA+plasminogen+aprotinin for 3 hours at 37°C and then studied the cleavage of HMWK by immunoblotting. As expected from our in vivo results, only tPA+plasminogen incubation induced HMWK cleavage (Figure 6A). This effect was blocked by aprotinin, confirming that HMWK cleavage is dependent on the proteolytic activity of plasmin. To study the kinetics of this effect, we incubated HMWK with plasmin and studied its cleavage at different points after incubation (from 0 to 24 hours). As shown in Figure 6B, plasmin rapidly (30 minutes) triggers HMWK cleavage in purified conditions (Figure 6B). Under these conditions, HMWK cleavage was complete after 3 hours of incubation. Then we investigated whether HMWK cleavage by plasmin induces bradykinin generation. We measured bradykinin generation by enzyme-linked immunosorbent assay in samples where HMWK has been cleaved by plasmin. As observed (Figure 6C), HMWK cleavage by plasmin led to bradykinin generation. Aprotinin completely prevented the generation of bradykinin. These results demonstrated that tPA, through plasminogen activation, leads to HMWK cleavage and bradykinin generation (Figure 6D).

Intravenous tPA infusion induces bradykinin generation in humans

As a consequence, we wanted to investigate whether a hyperfibrinolytic state could generate bradykinin through HMWK cleavage in humans. We needed a clinical situation in which we were able to measure HMWK and bradykinin concentrations before and after occurrence of a hyperfibrinolytic state. We decided to take advantage of tPA infusion in patients with ischemic stroke (supplemental Table 2). Cleavage of endogenous HMWK was measured in blood samples from a cohort (n = 8) of tPA-injected patients (Figure 7A).[25] First, we analyzed the cleavage of HMWK in those patients at different points before (0 hours) and after (1, 2, 12, and 24 hours; Figure 7B) tPA infusion. We observed that tPA infusion rapidly triggers HMWK cleavage (Figure 7C-E). Interestingly, the percentage of HMWK cleavage after thrombolysis differed between the patients, revealing individuals with almost complete HMWK cleavage (Figure 7C), and others with lower cleavage (Figure 7D). Nevertheless, all patients individually presented HMWK cleavage at the end of tPA infusion, and those levels were partly restored 24 hours after thrombolysis (individual data are presented in supplemental Figure 12). We also compared bradykinin levels before and 1 hour after thrombolysis by enzyme-linked immunosorbent assay in the same patient cohort. Our data demonstrate that tPA infusion in humans generates bradykinin in vivo, as higher plasmatic bradykinin levels were measured in all patients 1 hour after thrombolysis compared with before (n = 8; Figure 7F). Taken together, these results demonstrated that, in humans, an acute hyperfibrinolytic state induced by tPA infusion triggers HMWK cleavage and bradykinin generation.

Discussion

In the present study, we propose a mechanistic model by which hyperfibrinolysis induces BBB leakage in a plasmin- and bradykinin-dependent manner (Figure 6D). After hydrodynamic transfection of an expression vector encoding for tPA, we first demonstrated that mice produce and secrete active tPA from their liver to the circulation,

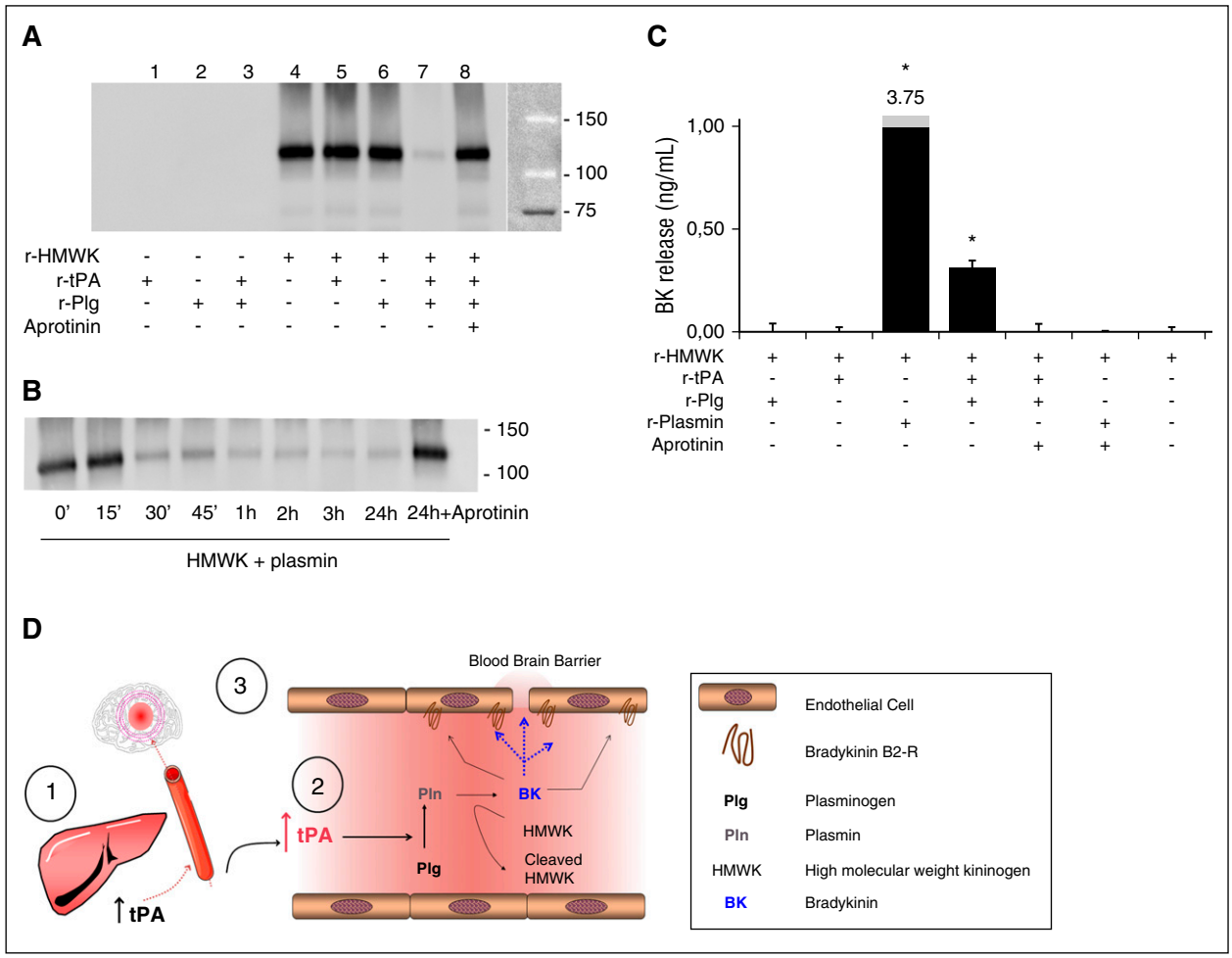

Figure 6. Plasminogen activation by tPA mediates bradykinin generation. (A) Representative HMWK western blot (120 KDa) after 3 hours of incubation, showing that plasminogen activation (by tPA+plasminogen) promotes HMWK cleavage and that this effect is a result of plasmin generation, as aprotinin blocked the effect. (B) Time-course of HMWK cleavage by plasmin. This cleavage was prevented by aprotinin. (C) Enzyme-linked immunosorbent assay bradykinin levels showing that either recombinant plasmin or generated plasmin (by tPA-dependent plasminogen activation) generate bradykinin by HMWK cleavage. This effect is prevented by aprotinin. All experiments were performed in triplicate. (D) Schematic representation of the mechanistic link between hydrodynamic transfection of tPA in the liver and subsequent BBB leakage. *$P < .05$ vs control.

thereby leading to a sustained hyperfibrinolytic state. Using this preclinical model, we demonstrated that hyperfibrinolysis induces BBB leakage by a plasmin-dependent generation of bradykinin and subsequent activation of B2 receptors. Moreover, we provided evidence that these results are clinically relevant by showing that tPA infusion promotes bradykinin generation in humans.

The pathophysiological mechanisms leading to hyperfibrinolysis remain poorly understood, and may vary according to the etiology. Nevertheless, in all clinical studies, the hyperfibrinolytic state was found to be the result of an increased level of profibrinolytic factors that is not (or not fully) compensated by an increased level of antifibrinolytic factors.[26] This imbalance triggers plasmin generation and leads to a severe bleeding tendency. Thus, by increasing the plasmatic level of tPA, our present preclinical model mimics human hyperfibrinolysis. This model could be useful for investigating the roles of hyperfibrinolysis on outcome in a number of diseases such as traumatic brain injury, multiple organ failure, anaphylaxia,[27] or acute promyelocytic leukemia.[28,29]

Although numerous studies have investigated the effects of tPA on the BBB, most of them have proposed plasminogen-independent mechanisms including overexpression of matrix metalloproteinases 2, 3, and 9[21] and activation/cleavage of either LRP[22,30] or platelet-derived growth factor.[31] However, other studies suggest multifactorial and probably plasminogen-dependent effects of tPA on the BBB,[32] as recently reviewed by Niego and Medcalf.[13] In the present study, we demonstrated that chronic tPA overexpression increases the permeability of the intact BBB by a plasminogen-dependent mechanism. This effect involves plasmin-dependent generation of bradykinin and subsequent activation of bradykinin B2 receptors. Therefore, blockade of plasmin generation (using antifibrinolytic drugs) or B2 receptors (using icatibant) prevents BBB disruption in mice presenting hyperfibrinolysis. These therapeutic strategies could be useful in patients presenting with hyperfibrinolysis to preserve the integrity of the BBB; for example, in individuals with liver cirrhosis, who present with high rates of spontaneous intracerebral hemorrhages. It is possible that chronic vs acute increases in tPA levels in the circulation act by different mechanisms. For instance, knowing that fibrinogen has been implicated in BBB impairment, we performed exploratory analyses that revealed that fibrinogen degradation occurs in human stroke during acute fibrinolysis, whereas no significant degradation occurs in hyperfibrinolytic mice (supplemental Figure 13).

Previous clinical and preclinical studies support the relevance of the present described mechanism. Indeed, in some patients,

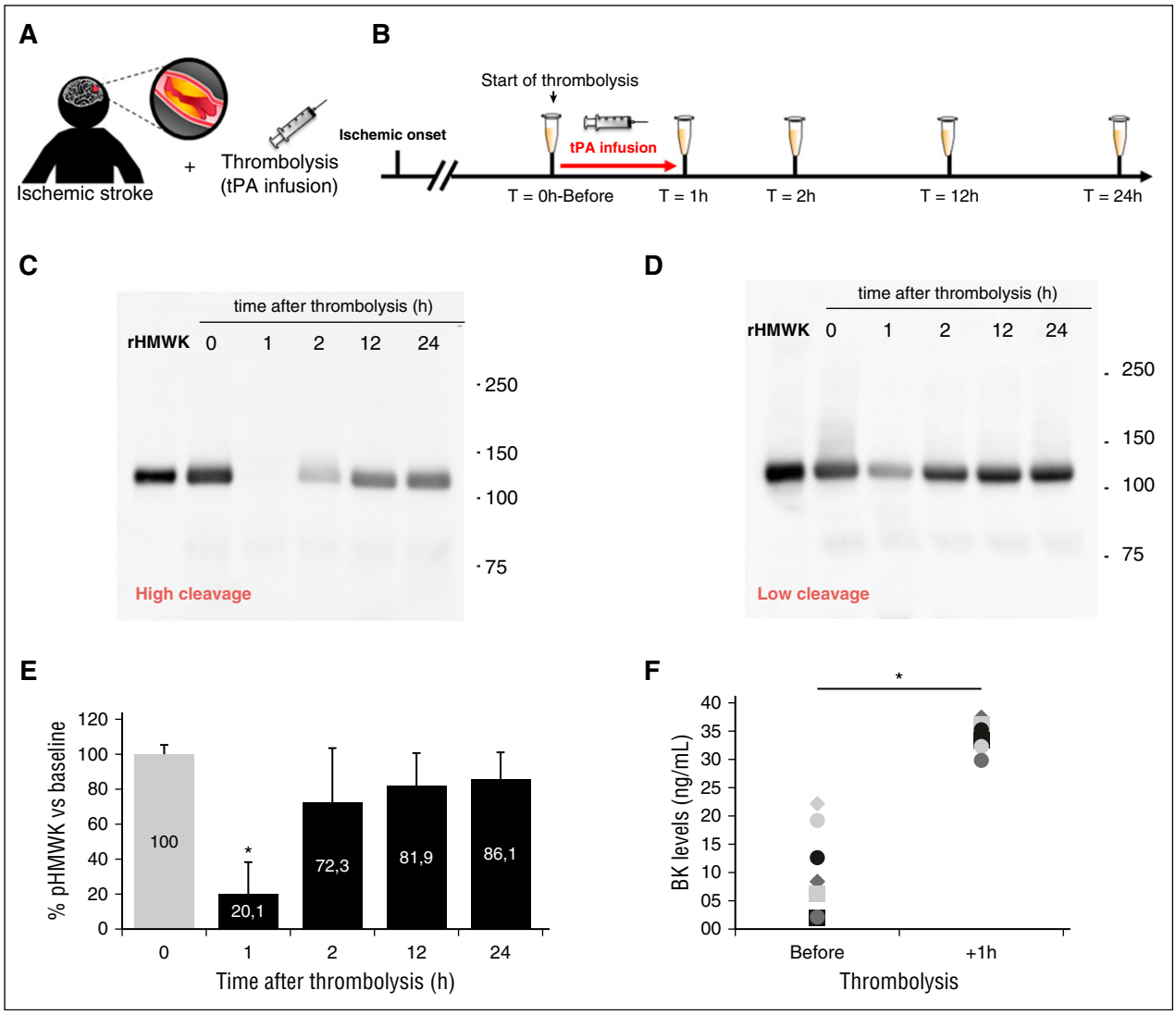

Figure 7. Acute intravenous tPA promotes bradykinin generation in patients with ischemic stroke. (A-B) Time-course of plasma samples collection in patients with ischemic stroke who received thrombolytic therapy. Blood samples were obtained at 0 (before), 1, 2, 12, and 24 hours after tPA infusion. (C-D) Representative western blots of plasmatic HMWK levels (120 KDa) in patients with stroke before and after tPA infusion, showing that plasmin generation promotes HMWK cleavage. Both high (B) and low (C) profiles of HMWK cleavage were found in the small cohort of patients with stroke. Recombinant HMWK was used as a reference. (E) Mean percentage of plasmatic HMWK levels in patients with stroke over time. Baseline levels were used to normalize samples (100%) (n = 8). (F) Quantification of bradykinin (BK) levels in those patients at the baseline level (before) and at the end of thrombolysis (+1 hour), showing that HMWK cleavage promotes bradykinin generation. *$P < .05$ vs control.

pharmacologically induced fibrinolysis induces angioedema, an infrequent but dramatic complication of thrombolysis involving massive fluid leakage from permeabilized vessels.[33] This complication occurs almost exclusively in patients taking angiotensinogen-converting enzyme inhibitors, an enzyme that is also responsible for bradykinin degradation.[34] Thus, in addition to our results, there are strong data demonstrating that plasmin induces bradykinin generation in humans. Moreover, previous studies demonstrated that bradykinin B2 receptor agonists induce BBB leakage in mice and rats.[24] Here, contrasting with previous reports on bradykinin effects in the brain that reported only transient BBB leakage, our results suggest that the hyperfibrinolysis-induced BBB leakage is sustained. It is tempting to speculate that the initial BBB leakage induced by bradykinin allows circulating tPA to enter the brain parenchyma, where it can exert further deleterious effects on BBB integrity and glutamatergic transmission. This effect, among others, could also explain why hyperfibrinolytic mice present behavioral changes and no significant brain edema. Interestingly, elevated bradykinin generation has been recently described in the blood of patients with Alzheimer disease,[35] who also present significant and sustained BBB impairment, without significant brain edema.[36]

The differential response between BBB and blood–spinal cord barrier (BSCB) we observed may be explained by several structural discrepancies that exist between the 2 barriers. Previous studies demonstrated that B2 receptor antagonists alleviate BSCB leakage after spinal cord injury,[37] suggesting bradykinin is also involved in BSCB disruption. Nevertheless, our present results demonstrate that hyperfibrinolysis alone is not sufficient to increase BSCB permeability for large proteins. There may be differences in the number of endothelial receptors for plasminogen in brain and spinal cord vessels,[38] leading to more efficient plasmin generation in the brain compared with in the spinal cord. Indeed, brain endothelial cells generate larger amounts of plasmin in the presence of tPA compared with other endothelial cell types.[38] This discrepancy may also explain

why spinal cord hemorrhage after thrombolytic therapy is a very infrequent complication. Because the permeability of skin capillaries also appears to be influenced by hyperfibrinolysis, further studies are needed to characterize endothelial cell properties (such as bradykinin B2 receptor expression) that make them responsive to hyperfibrinolysis.

In contrast to spinal cord hemorrhage, symptomatic intracranial hemorrhage is a relatively frequent complication of thrombolytic therapy (~1% for myocardial infarction and ~5% for ischemic stroke), inducing a dramatically high mortality rate (~50%).[39] Our results suggest that B2 receptor antagonists may be of interest to prevent BBB disruption and potentially reduce the hemorrhage rate in tPA-treated patients. In our small cohort of patients with ischemic stroke, none of them presented hemorrhagic transformations. Because of the small number of samples available, we cannot come to a conclusion on the role of bradykinin generation in stroke outcome. Moreover, there are conflicting reports on the role of bradykinin B1 and B2 receptors during ischemic stroke.[40-42] Because B2 receptors also display crucial roles in neuronal survival,[43] the resulting effect of icatibant on stroke outcome in thrombolysed patients deserves further investigation. Although our data revealed the production of bradykinin after tPA infusion in patients with stroke, we cannot associate this phenomenon with a risk for hemorrhagic transformations. A study performed in a larger cohort, including patients with stroke who do not benefit from tPA treatment, will be necessary to confirm our results. Moreover, in the condition of hyperfibrinolysis (including associated conditions such as trauma or stroke), other mechanisms could be at play and also influence vascular permeability.

It is important to acknowledge that the measurements in humans were performed with blood sampled using standard procedures. Therefore, degradation of bradykinin could have occurred after blood sampling, and thus the plasmatic levels of bradykinin may be altered. Despite this limitation, as we measured bradykinin levels before and after fibrinolysis and used the same processing methods for all samples, we can conclude that bradykinin levels were higher after fibrinolysis. Moreover, the measured bradykinin concentrations were within the range of previously published studies.[44]

Overall, we provide here a relevant experimental model of hyperfibrinolysis to conduct further studies on this disorder. In addition, our study provides evidence in mice that hyperfibrinolysis induces BBB leakage in a plasmin- and bradykinin–B2-receptor–dependent manner. Accordingly, tPA infusion in patients with stroke also leads to the generation of bradykinin. Therefore, we propose that antifibrinolytic treatments or B2 receptor antagonists are interesting tools to preserve vascular integrity in patients presenting with hyperfibrinolysis.

Acknowledgments

This work was supported by INSERM, the Conseil Régional de Basse-Normandie, and the Eranet-ProteA Program (2011-2014).

Authorship

Contribution: O.A.M.-C., S.M.d.L., D.V., and M.G. designed the study and wrote the manuscript; O.A.M.-C., S.M.d.L., I.B., C.O., M.P., A.A., and M.G. performed experiments and analyzed the data; I.B., C.O., Y.F., Y.H., and L.L. participated in the development of the experimental model and reviewed the manuscript; and J.M. provided human samples and reviewed the manuscript;

Conflict-of-interest disclosure: The authors declare no competing financial interests.

Correspondence: Maxime Gauberti, INSERM UMR-S U919, Université de Caen Basse-Normandie, GIP Cyceron, Bd H. Becquerel, BP5229, 14074 Caen, France; e-mail: gauberti@cyceron.fr; and Denis Vivien, INSERM UMR-S U919, Université de Caen Basse-Normandie, GIP Cyceron, Bd H. Becquerel, BP5229, 14074 Caen, France; e-mail: vivien@cyceron.fr.

References

1. Raza I, Davenport R, Rourke C, et al. The incidence and magnitude of fibrinolytic activation in trauma patients. *J Thromb Haemost.* 2013; 11(2):307-314.
2. Rijken DC, Kock EL, Guimarães AH, et al. Evidence for an enhanced fibrinolytic capacity in cirrhosis as measured with two different global fibrinolysis tests. *J Thromb Haemost.* 2012; 10(10):2116-2122.
3. Schöchl H, Cadamuro J, Seidl S, et al. Hyperfibrinolysis is common in out-of-hospital cardiac arrest: results from a prospective observational thromboelastometry study. *Resuscitation.* 2013;84(4):454-459.
4. Breen KA, Grimwade D, Hunt BJ. The pathogenesis and management of the coagulopathy of acute promyelocytic leukaemia. *Br J Haematol.* 2012;156(1):24-36.
5. Shakur H, Roberts I, Bautista R, et al; CRASH-2 trial collaborators. Effects of tranexamic acid on death, vascular occlusive events, and blood transfusion in trauma patients with significant haemorrhage (CRASH-2): a randomised, placebo-controlled trial. *Lancet.* 2010; 376(9734):23-32.
6. Roullet S, Freyburger G, Labrouche S, et al. Hyperfibrinolysis during liver transplantation is associated with bleeding. *Thromb Haemost.* 2015; 113(5):1145-1148.
7. Marx I, Christophe OD, Lenting PJ, et al. Altered thrombus formation in von Willebrand factor-deficient mice expressing von Willebrand factor variants with defective binding to collagen or GPIIbIIIa. *Blood.* 2008;112(3):603-609.
8. von Drygalski A, Furlan-Freguia C, Mosnier LO, Yegneswaran S, Ruf W, Griffin JH. Infrared fluorescence for vascular barrier breach in vivo–a novel method for quantitation of albumin efflux. *Thromb Haemost.* 2012;108(5): 981-991.
9. Jaffer H, Adjei IM, Labhasetwar V. Optical imaging to map blood-brain barrier leakage. *Sci Rep.* 2013;3:3117.
10. Lopez-Atalaya JP, Roussel BD, Levrat D, et al. Toward safer thrombolytic agents in stroke: molecular requirements for NMDA receptor-mediated neurotoxicity. *J Cereb Blood Flow Metab.* 2008;28(6):1212-1221.
11. Nicole O, Docagne F, Ali C, et al. The proteolytic activity of tissue-plasminogen activator enhances NMDA receptor-mediated signaling. *Nat Med.* 2001;7(1):59-64.
12. Parcq J, Bertrand T, Baron AF, Hommet Y, Anglès-Cano E, Vivien D. Molecular requirements for safer generation of thrombolytics by bioengineering the tissue-type plasminogen activator A chain. *J Thromb Haemost.* 2013;11(3): 539-546.
13. Niego B, Medcalf RL. Plasmin-dependent modulation of the blood-brain barrier: a major consideration during tPA-induced thrombolysis? *J Cereb Blood Flow Metab.* 2014;34(8): 1283-1296.
14. Vivien D, Gauberti M, Montagne A, Defer G, Touzé E. Impact of tissue plasminogen activator on the neurovascular unit: from clinical data to experimental evidence. *J Cereb Blood Flow Metab.* 2011;31(11):2119-2134.
15. Gauberti M, Montagne A, Quenault A, Vivien D. Molecular magnetic resonance imaging of brain-immune interactions. *Front Cell Neurosci.* 2014; 8:389.
16. Montagne A, Gauberti M, Macrez R, et al. Ultra-sensitive molecular MRI of cerebrovascular cell activation enables early detection of chronic central nervous system disorders. *Neuroimage.* 2012;63(2):760-770.
17. Gauberti M, Montagne A, Marcos-Contreras OA, Le Béhot A, Maubert E, Vivien D. Ultra-sensitive molecular MRI of vascular cell adhesion molecule-1 reveals a dynamic inflammatory penumbra after strokes. *Stroke.* 2013;44(7):1988-1996.
18. Belliere J, Martinez de Lizarrondo S, Choudhury RP, et al. Unmasking Silent Endothelial Activation in the Cardiovascular System Using Molecular Magnetic Resonance Imaging. *Theranostics.* 2015;5(11):1187-1202.

19. Mannaioni G, Orr AG, Hamill CE, et al. Plasmin potentiates synaptic N-methyl-D-aspartate receptor function in hippocampal neurons through activation of protease-activated receptor-1. *J Biol Chem.* 2008;283(29):20600-20611.
20. Suzuki Y, Nagai N, Umemura K, Collen D, Lijnen HR. Stromelysin-1 (MMP-3) is critical for intracranial bleeding after t-PA treatment of stroke in mice. *J Thromb Haemost.* 2007;5(8): 1732-1739.
21. Wang X, Lee SR, Arai K, et al. Lipoprotein receptor-mediated induction of matrix metalloproteinase by tissue plasminogen activator. *Nat Med.* 2003;9(10):1313-1317.
22. Yepes M, Sandkvist M, Moore EG, Bugge TH, Strickland DK, Lawrence DA. Tissue-type plasminogen activator induces opening of the blood-brain barrier via the LDL receptor-related protein. *J Clin Invest.* 2003;112(10):1533-1540.
23. Carmo AA, Costa BR, Vago JP, et al. Plasmin induces in vivo monocyte recruitment through protease-activated receptor-1-, MEK/ERK-, and CCR2-mediated signaling. *J Immunol.* 2014; 193(7):3654-3663.
24. Borlongan CV, Emerich DF. Facilitation of drug entry into the CNS via transient permeation of blood brain barrier: laboratory and preliminary clinical evidence from bradykinin receptor agonist, Cereport. *Brain Res Bull.* 2003;60(3):297-306.
25. Briens A, Gauberti M, Parcq J, Montaner J, Vivien D, Martinez de Lizarrondo S. Nano-zymography Using Laser-Scanning Confocal Microscopy Unmasks Proteolytic Activity of Cell-Derived Microparticles. *Theranostics.* 2016;6(5):610-626.
26. Gando S. Hemostasis and thrombosis in trauma patients. *Semin Thromb Hemost.* 2015;41(1): 26-34.
27. Truong HT, Browning RM. Anaphylaxis-induced hyperfibrinolysis in pregnancy. *Int J Obstet Anesth.* 2015;24(2):180-184.
28. Jácomo RH, Santana-Lemos BA, Lima AS, et al. Methionine-induced hyperhomocysteinemia reverts fibrinolytic pathway activation in a murine model of acute promyelocytic leukemia. *Blood.* 2012;120(1):207-213.
29. Xie R, Gao C, Li W, et al. Phagocytosis by macrophages and endothelial cells inhibits procoagulant and fibrinolytic activity of acute promyelocytic leukemia cells. *Blood.* 2012; 119(10):2325-2334.
30. Polavarapu R, Gongora MC, Yi H, et al. Tissue-type plasminogen activator-mediated shedding of astrocytic low-density lipoprotein receptor-related protein increases the permeability of the neurovascular unit. *Blood.* 2007;109(8): 3270-3278.
31. Su EJ, Fredriksson L, Geyer M, et al. Activation of PDGF-CC by tissue plasminogen activator impairs blood-brain barrier integrity during ischemic stroke. *Nat Med.* 2008;14(7):731-737.
32. Niego B, Freeman R, Puschmann TB, Turnley AM, Medcalf RL. t-PA-specific modulation of a human blood-brain barrier model involves plasmin-mediated activation of the Rho kinase pathway in astrocytes. *Blood.* 2012;119(20): 4752-4761.
33. Hill MD, Lye T, Moss H, et al. Hemi-orolingual angioedema and ACE inhibition after alteplase treatment of stroke. *Neurology.* 2003;60(9): 1525-1527.
34. Molinaro G, Gervais N, Adam A. Biochemical basis of angioedema associated with recombinant tissue plasminogen activator treatment: an in vitro experimental approach. *Stroke.* 2002;33(6): 1712-1716.
35. Zamolodchikov D, Chen ZL, Conti BA, Renné T, Strickland S. Activation of the factor XII-driven contact system in Alzheimer's disease patient and mouse model plasma. *Proc Natl Acad Sci USA.* 2015;112(13):4068-4073.
36. Montagne A, Barnes SR, Sweeney MD, et al. Blood-brain barrier breakdown in the aging human hippocampus. *Neuron.* 2015;85(2):296-302.
37. Sharma HS. A bradykinin BK2 receptor antagonist HOE-140 attenuates blood-spinal cord barrier permeability following a focal trauma to the rat spinal cord. An experimental study using Evans blue, [131]I-sodium and lanthanum tracers. *Acta Neurochir Suppl (Wien).* 2000;76:159-163.
38. Kwaan HC, Wang J, Weiss I. Expression of receptors for plasminogen activators on endothelial cell surface depends on their origin. *J Thromb Haemost.* 2004;2(2):306-312.
39. Karaszewski B, Houlden H, Smith EE, et al. What causes intracerebral bleeding after thrombolysis for acute ischaemic stroke? Recent insights into mechanisms and potential biomarkers. *J Neurol Neurosurg Psychiatry.* 2015;86(10):1127-1136.
40. Gauberti M, Martinez de Lizarrondo S, Orset C, Vivien D. Lack of secondary microthrombosis after thrombin-induced stroke in mice and non-human primates. *J Thromb Haemost.* 2014;12(3): 409-414.
41. Su J, Cui M, Tang Y, Zhou H, Liu L, Dong Q. Blockade of bradykinin B2 receptor more effectively reduces postischemic blood-brain barrier disruption and cytokines release than B1 receptor inhibition. *Biochem Biophys Res Commun.* 2009;388(2):205-211.
42. Langhauser F, Göb E, Kraft P, et al. Kininogen deficiency protects from ischemic neurodegeneration in mice by reducing thrombosis, blood-brain barrier damage, and inflammation. *Blood.* 2012;120(19):4082-4092.
43. Martins AH, Alves JM, Perez D, et al. Kinin-B2 receptor mediated neuroprotection after NMDA excitotoxicity is reversed in the presence of kinin-B1 receptor agonists. *PLoS One.* 2012;7(2): e30755.
44. Kunz M, Nussberger J, Holtmannspötter M, Bitterling H, Plesnila N, Zausinger S. Bradykinin in blood and cerebrospinal fluid after acute cerebral lesions: correlations with cerebral edema and intracranial pressure. *J Neurotrauma.* 2013; 30(19):1638-1644.